physica status solidi
pss
www.pss-journals.com
reprint

WILEY-VCH

Phys. Status Solidi C **10**, No. 11, 1644–1647 (2013) / **DOI** 10.1002/pssc.201300235

physica status solidi pss c
www.pss-c.com
current topics in solid state physics

Band structures of Si/InGaP heterojunctions by using surface-activated bonding

Jianbo Liang[*], **Masashi Morimoto, Shota Nishida, and Naoteru Shigekawa**

Department of Electrical Engineering, Osaka City University, Sugimoto 3-3-138, Sumiyoshi, 558-8585 Osaka, Japan

Received 21 June 2013, revised 22 July 2013, accepted 26 August 2013
Published online 23 September 2013

Keywords surface-activated bonding, Si/InGaP heterojunctions, notch, conduction-band discontinuity

* Corresponding author: e-mail liang@elec.eng.osaka-cu.ac.jp, Phone: +81 6 6605 2973, Fax: +81 6 6605 2973

The band structure of *p*-Si/*n*-InGaP heterojunctions fabricated by using surface-activated bonding (SAB) was investigated by measuring their current-voltage (*I-V*) and capacitance-voltage (*C-V*) characteristics. The *I-V* characteristics of *p*-Si/*n*-InGaP junctions showed rectifying properties similarly to *p*-Si/*n*-GaAs junctions. The conduction band discontinuity of the *p*-Si/*n*-InGaP junctions was determined to be 0.41 eV from *C-V* measurements, which indicated that the Si/InGaP junctions revealed the type-I band line-up in contrast to the Si/GaAs junctions.

© 2013 WILEY-VCH Verlag GmbH & Co. KGaA, Weinheim

1 Introduction Direct bonding of semiconductor materials has been studied by several groups [1, 2]. This method has been employed for forming a variety of semiconductor junctions [3-6]. The process for removing native oxide layers on the bonding surfaces is essential prior to forming the above-cited junctions. Furthermore, processes at higher temperatures during and/or after bonding are required for realizing junctions with better electrical characteristics [5, 6]. Such high-temperature processes, however, might cause the diffusion of impurities through the interfaces or mechanical deficits due to the difference in the thermal expansion coefficients of bonded substrates, which are assumed to limit the area of applications of the direct wafer bonding.

Surface-activated bonding (SAB) is a method to achieve bonding at room temperature [7-12]. In the process, surfaces of substrates are activated by the fast atom beams of Ar and subsequently brought into contact in a vacuum. SAB, consequently, has enabled us to bond substrates without heating [7]. This method has a significant advantage of avoiding undesirable heat loads for heat sensitive electronics devices. SAB has been found to be applicable in chip-size and wafer-level optoelectronic and micro electro mechanical systems packaging. The prime concern in relevant research has been the mechanical and structural properties of junctions [9, 10] although current-voltage (*I-V*) characteristics of SAB-based Si/Si, Si/InP, and Si/GaAs junctions were reported [8, 11, 12].

In this work, the *p*-Si/*n*-InGaP junctions were fabricated by using SAB. The InGaP layers were lattice-matched to GaAs. Given that the band gap of lattice-matched InGaP (1.88 eV at room temperature) is larger than that of GaAs (1.42 eV), InGaP/Si junctions might be useful as tunneling junction in tandem solar cells. We examined their electrical properties by current-voltage (*I-V*) and capacitance-voltage (*C-V*) measurements and discussed their energy-band stuctures with those for *p*-Si/*n*-GaAs junctions [12].

2 Experimental procedure We employed B-doped (100) *p*-Si substrates and Si-doped *n*-InGaP layers epitaxially-grown on *n*-GaAs substrates. The nominal carrier concentration in *n*-InGaP layers was 1×10^{18} cm^{-3}. The hall measurements at room temperature revealed that the resistivity and carrier concentration were 0.1 Ω·cm and 2.4×10^{17} cm^{-3} for the *p*-Si substrates. We bonded the *p*-Si substrates and *n*-InGaP layers to each other by using SAB [7-12], evaporated Al/Ni/Au and AuGe/Ni/Ti/Au multilayers on the backside of *p*-Si and *n*-GaAs substrates, respectively, and annealed them at 400 °C for 60 s so that the ohmic contacts were achieved. All samples were then diced into 4 mm^2 pieces. Their *I-V* characteristics were measured using an Agilent B2902A Precision Measurement Unit. Their *C-V* characteristics were measured using an Agilent E4980A Precision Impedance Analyzer at room temperature. An FE-SEM facility (JEOL

© 2013 WILEY-VCH Verlag GmbH & Co. KGaA, Weinheim

JSM6500F) was employed for the cross-sectional characterizations for sides formed by dicing.

The p-Si/n-GaAs junctions used as reference samples were fabricated in similar manners. The carrier concentrations in the p-Si and the n-GaAs were 2.4 × 10^{17} cm^{-3} and 1.1 × 10^{18} cm^{-3}, respectively.

3 Results Figure 1 shows an FE-SEM image of the cross section of p-Si/n-InGaP junctions. A straight line can be clearly recognized at the centre of the sample. This line corresponds to the interface between Si and InGaP. Some cracks were observed mainly in the side of InGaP layers at the cross-sectional surface, which are attributed to dicing damage.

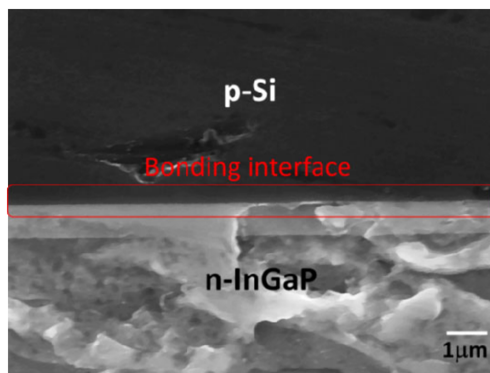

Figure 1 FE-SEM cross-sectional image of the interface of Si/InGaP.

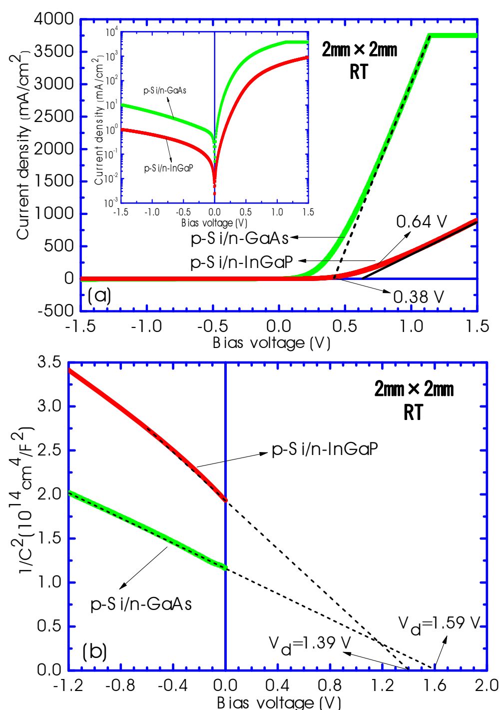

Figure 2 (a) I-V and (b) C-V characteristics of SAB-based p-Si/n-InGaP junctions at room temperature. Results for p-Si/n-GaAs junctions are also shown for comparison.

The I-V characteristics of the p-Si/n-InGaP junctions measured at room temperature are shown in Fig. 2(a). Those of the p-Si/n-GaAs junctions were also shown for comparison. It was found that both the curves revealed rectifying properties similarly to those in conventional pn junctions. The turn-on voltages were found to be 0.64 and 0.38 V for the p-Si/n-InGaP and the p-Si/n-GaAs junctions, respectively. The inset shows the semi-log plot of I-V characteristics of the p-Si/n-InGaP and the p-Si/n-GaAs junctions. It is noteworthy that the magnitude of the current increased as the junctions were more deeply reverse biased for both the p-Si/n-InGaP and the p-Si/n-GaAs junctions. In addition, the magnitude of the current of the p-Si/n-GaAs junctions is larger than that of the p-Si/n-InGaP junctions for reverse bias voltages.

The $1/C^2$-V characteristics of the p-Si/n-InGaP junctions measured at a frequency of 100 kHz are shown in Fig. 2(b). It exhibits characteristics in which $1/C^2$ is approximately a linear function of the applied voltage. However, a decrease in slope with increasing reverse bias was very noted. Although a slight warp was observed in the characteristics, the diffusion potential was found to be ~ 1.39 V by linearly extrapolating $1/C^2$ for the bias voltages between -0.6 and 0 V to zero. The $1/C^2$-V characteristics of the p-Si/n-GaAs junctions are also shown in this figure for comparison. The diffusion potential of the p-Si/n-GaAs junctions was found to be ~ 1.59 V.

The I-V characteristics of p-Si/n-InGaP junctions measured at varied temperatures are shown in Fig. 3. It is noteworthy that the magnitude of the current increased as the junctions were more deeply reverse biased. Furthermore, the magnitude of the current increased with increasing the temperatures. We also find that the slope of the current for reverse-bias voltages is almost invariant to temperature.

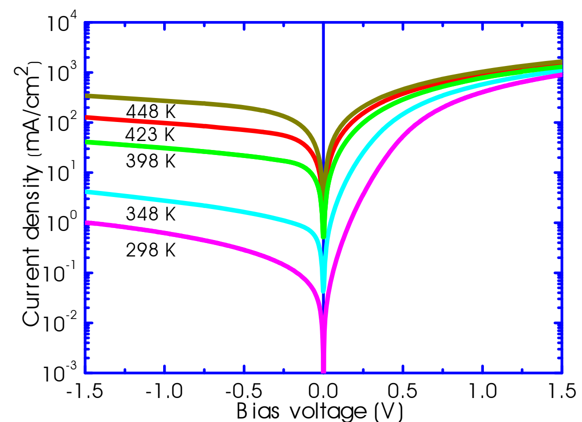

Figure 3 I-V characteristics of p-Si/n-InGaP junctions measured at varied temperature.

4 Discussion The diffusion potential V_d in p-Si/n-InGaP junctions, which is given by the difference in the

© 2013 WILEY-VCH Verlag GmbH & Co. KGaA, Weinheim

work functions between *p*-Si and *n*-InGaP(*n*-GaAs), is expressed as

$$qV_d = E_{gp} + \Delta E_c + \delta_n - \delta_p. \quad (1)$$

where q is the elementary charge, E_{gp} is the energy gap of *p*-Si, ΔE_c is the conduction-band discontinuity, and δ_p and δ_n refer to the position of the Fermi energies relative to the valence-band maximum in *p*-Si and that relative to the conduction-band minimum in *n*-InGaP, respectively.

Using Eq. (1), ΔE_c is estimated to be 0.41 eV for the *p*-Si/*n*-InGaP junctions. Their valence-band discontinuity is, consequently, found to be 0.35 eV. The energy-band diagram at zero-bias voltage based on these estimations is shown in Fig. 4(a).

The energy-band diagram of the *p*-Si/*n*-GaAs junctions, which was obtained in similar manners, is shown in Fig. 4(b) for comparison. Where ΔE_v is the valence band discontinuity, and X_n and X_p are the depletion width of n-GaAs or InGaP and p-Si in the *p*-Si/*n*-GaAs and *p*-Si/*n*-InGaP junctions. We find that the energy-band diagram of the *p*-Si/*n*-InGaP junctions reveals type-I features although type-II features are apparent in that of the *p*-Si/*n*-GaAs junctions. These findings are in contradiction with a previous report for the energy-band profile of InGaP/GaAs junctions, which showed ΔE_c of 0.11 eV [13]. The electric dipole possibly formed at the bonding interfaces might explain the contradiction [14-16].

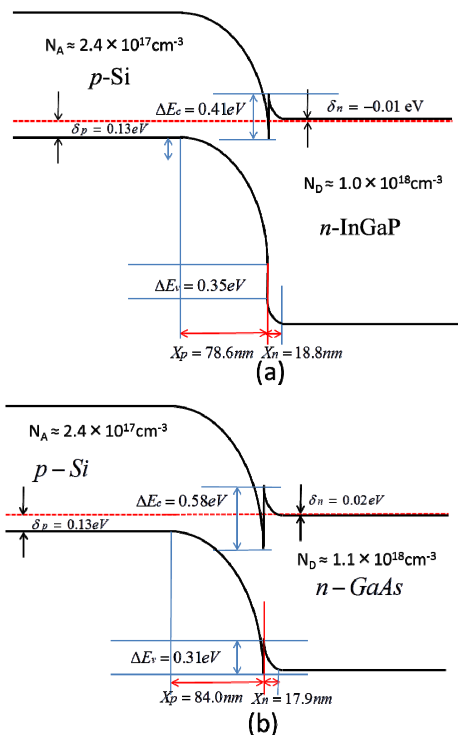

Figure 4 The schematic energy-band diagram of (a) p-Si/n-InGaP and (b) p-Si/n-GaAs junctions.

We found that the diffusion potential is surprisingly larger compared with the turn-on voltages and the magnitude of the current increased for larger reverse bias voltage for both of the *p*-Si/*n*-InGaP and the *p*-Si/*n*-GaAs junctions. Similar results were reported for the *p*-GaAs/*n*-GaN and the *p*-SiC/*n*-GaN junctions fabricated by wafer fusion, which were attributed to the scheme of trap-assisted tunneling [17-19].

Actually the fact that in the *I-V* characteristics of the *p*-Si/*n*-InGaP junctions the slope of the current for reverse bias voltages in the semi-log scale is not sensitive to the ambient temperature (Fig. 3) suggests that the tunneling process dominates the electrical transport properties across the interfaces. The analysis shows that the energy of the traps is estimated to be ~ 0.08 eV. The energy of the traps is close to that in the *p*-Si/*n*-GaAs junctions that we previously reported (0.1 eV).

One possible origin of the traps is damages formed on the bonding surfaces during the Ar plasma irradiation in the SAB process. Formation of amorphous layers due to SAB supports this model [9, 12]. Another explanation is that the notch, or the conduction-band discontinuity, formed at the Si/InGaP and Si/GaAs interfaces might play a role of traps. Note that the notch in AlGaAs heterojunctions reportedly can act as a trap [20]. The difference in the depth of the notch between the Si/InGaP (0.41 eV) and Si/GaAs (0.58 eV) junctions might be related to the energies of traps obtained from the *I-V* characteristics for the respective *pn* junctions.

The warp in the $1/C^2$-V characteristics of the *p*-Si/*n*-InGaP junctions might be explained by considering the mobile charges trapped at the interface during the tunneling [21, 22]. In addition, the slope decreased with increasing reverse biased in the $1/C^2$-V characteristics for the p-Si/n-InGaP junctions which is similar to those for n-Ge/p-Si vapor grown diode [23]. The considerable electric dipole or charged states may be formed at the bonding interfaces which may affect the $1/C^2$-V characteristics. For the p-Si/n-GaAs junctions, the interface states also may be formed at the interface, but its effects is relatively small compared with the p-Si/n-InGaP junctions because the value of $1/C^2$ at the bias of 0 V is consistent with the depletion width shown in Fig. 4(b).

5 Conclusion We successfully fabricated *p*-Si/*n*-InGaP junctions by using SAB and examined their energy-band structure in comparison with that of *p*-Si/*n*-GaAs junctions. The energy-band structure of *p*-Si/*n*-InGaP junctions, which we obtained from their *C-V* characteristics, showed type-I feature in contrast to that of *p*-Si/*n*-GaAs junctions. The contribution of traps was observed in the *I-V* characteristics of both of the junctions, which might be attributed to the damage due to the Ar plasma irradiation or the notch in the conduction band profile of the respective junctions.

© 2013 WILEY-VCH Verlag GmbH & Co. KGaA, Weinheim

Acknowledgements This work was supported by "Creative research for clean energy generation using solar energy" project in Core Research for Evolutional Science and Technology (CREST) programs of the Japan Science and Technology Agency (JST).

References

[1] Q. Tong, G. Cha, R. Gafiteanu, and U. Gösele, J. Microelectromech. Syst. **3**, 29 (1994).
[2] M. K. Weldon, Y. J. Chabal, D. R. Hamann, S. B. Christman, and E. E. Chaban, J. Vac. Sci. Technol. B **14**, 3095 (1996).
[3] S. Bengtsson and O. Engström, J. Appl. Phys. **66**, 3095 (1989).
[4] M. Shimbo, K. Furukawa, K. Fukuda, and K. Tanzawa, J. Appl. Phys. **31**, 3483 (1992).
[5] F. Shi, K.-L. Chang, J. Epple, C.-F. Xu, K. Y. Cheng, and K. C. Hsieh, J. Appl. Phys. **92,** 7544 (2002).
[6] K. Tanabe, A. F. I. Morral, and H. A. Atwater, Appl. Phys. Lett. **89**, 102106 (2006).
[7] Q. Y. Tong, R. Gafiteanu, and U. Gösele, Jpn. J. Appl. Phys. **31**, 3483 (1992).
[8] H. Takagi, K. Kikuchi, R. Maeda, T. R. Chung, and T. Suga, Appl. Phys. Lett. **68**, 2222 (1996).
[9] N. Shigekawa, N. Watanabe, and E. Higurashi, Proc. 3rd Int. IEEE Workshop on Low-temperature Bonding for 3D Intergration, Tokyo, Japan, 22-23 May 2012, edited by T. Suga, H. Takagi, and E. Higurashi, pp.109-112.
[10] H. Takagi and R. Maeda, J. Micromech. Microeng. **15**, 290 (2005).
[11] M. M. R. Howlader, T. Watanabe, and T. Suga, J. Appl. Phys. **91**, 3062 (2002).
[12] J. Liang, T. Miyazaki, M. Morimoto, S. Nishida, N. Watanabe, and N. Shigekawa, Appl. Phys. Express **6**, 021801 (2013).
[13] M. A. Haase, M. J. Hafich, and G. Y. Robinson, Appl. Phys. Lett. **58**, 104574 (1991).
[14] M. Peressi, L. Colombo, R. Resta, S. Baroni, and A. Baldereschi, Phys. Rev. B **48**, 12047 (1993).
[15] S. A. Chambers, Y. Liang, Z. Yu, R. Droopad, and J. Ramdani, J. Vac. Sci. Technol. A **19**, 934 (2001).
[16] L. Sorba, G. Bratina, A. Antonini, and A. Fraciosi, Phys. Rev. B **46**, 6834 (1992).
[17] J. T. Torvik, C. Qiu, M. Leksono, and J. I. Pankove, Appl. Phys. Lett. **72**, 945 (1998).
[18] E. Danielsson, C. M.Zetterling, M. Östling, A. Nikolaev, I. P. Nikitina, and V. Dmitriev, IEEE Trans. Electron Devices **48**, 444 (2001).
[19] O. Mitrofanov and M. Manfra, Appl. Phys. Lett. **84**, 422 (2004).
[20] I. B. Peterescu-Prahova, P. Mihailovici, C. Nache, C. Constantinescu, and W. Haecker, IEEE. Trans. Electron Devices **ED-23**, 37 (1976).
[21] J. P. Donnelly and A. G. Milnes, IEEE Trans. Electron Devices **14**, 63 (1967).
[22] C. Lian, H. G. Xing, Y. Chang, and N. Fichtenbaum, Appl. Phys. Lett. **93**, 112103 (2008).
[23] J. P. Donnelly and A. G. Milnes IEEE Trans. Electron Devices **ED-14**, 63 (1967).

© 2013 WILEY-VCH Verlag GmbH & Co. KGaA, Weinheim